The effect of temperature on wear and friction of a high strength steel in fretting [☆]

S.R. Pearson *, P.H. Shipway, J.O. Abere, R.A.A. Hewitt

Division of Materials, Mechanics and Structures and University Technology Centre in Gas Turbine Transmission Systems, The Faculty of Engineering, University of Nottingham, University Park, Nottingham NG7 2RD, UK

ARTICLE INFO

ABSTRACT

This paper investigates the effect of temperature (between 24 °C and 450 °C) on the wear rate and friction coefficient of a high strength alloy steel (Super-CMV) in gross sliding fretting in air. It was found that whilst there was significant loss of material from the contact during fretting at room temperature, the overall loss of material from the contact had become negative even with a modest increase in temperature to 85 °C. At temperatures greater than 85 °C, negative wear was maintained, with the coefficient of friction dropping monotonically with increasing temperature up to 450 °C. It is proposed that the changes in wear rate and friction coefficient were due to changes in the way that the oxide particles sintered to form a protective debris bed, with sintering of the oxide debris particles at these low temperatures being promoted by the nano-scale at which the oxide debris is formed.

© 2013 CERN. The Authors. Published by Elsevier B.V. All rights reserved.

1. Introduction

Fretting is the oscillatory motion of two contacting bodies at small displacement amplitudes; the relative motion creates material damage (which can be broadly classified into wear and fatigue). The behaviour of a fretting contact is known to depend critically upon the debris which is formed during the process, and in particular its rate of creation and ejection from the contact and the properties of any debris which is retained in the contact.

Fretting of mating components is encountered in many industrial contexts, with these contacts existing in a range of environments, including across a range of temperatures. Temperature has a strong influence on many physical systems through its influence on thermodynamics (for example, influencing which phases are favoured in a system), kinetics (for example, influencing the rate of oxidation and sintering) and material properties (for example, influencing stiffness and strength of solids). In light of this, it can be assumed that the formation of debris beds within a fretting contact depends upon many attributes which are influenced by temperature; accordingly, a body of research exists which has examined the effects of elevated temperature on the tribology of dry fretting steel contacts [1–6].

In general terms, as the temperature is increased, the wear rate and coefficient of friction (COF) are typically observed to decrease significantly over a relatively narrow range of temperature, commonly referred to as the transition temperature. Reductions of over an order of magnitude in the wear rate of both medium carbon and stainless steels (with associated decreases in the COF of approximately 20%–30%) have been observed [1,2]. Similar behaviour is widely reported in the literature relating to reciprocating sliding wear at elevated temperatures [7–11], indicating that changes in mechanisms controlling the contact tribology are not specific to fretting.

Hurricks [4,5] related the transition temperature to a change in oxidation from logarithmic to parabolic growth (related to the growth of a sufficiently thick protective surface oxide film) and to the growing predominance of Fe_3O_4 within the oxide film (rather than $\alpha-Fe_2O_3$ which was thought to be the dominant oxide below the transition temperature). This is supported by Kayaba and Iwabuchi [2], who similarly associated the reduction in wear and COF with increasing temperature with the change in oxide from $\alpha-Fe_2O_3$ to Fe_3O_4. Under sliding wear conditions, researchers have also attributed the reduction in wear and COF observed at elevated temperatures to the formation of Fe_3O_4 which is thought to adhere more strongly to the surface and act as a better solid lubricant than $\alpha-Fe_2O_3$ [11,12].

Later work has emphasized the mechanical role of the debris rather than the properties of the particular oxide or the rate at which a surface oxide film may form. Godet [13] outlined the importance of the behaviour of debris interposed between the primary wearing surfaces in terms of a 'third-body-approach'. When the wearing faces of a contact are separated by a layer of

debris, then the debris layer itself can protect the primary surfaces by supporting the bearing load and providing a means through which the shear displacement between the faces may be accommodated [14]. Experimentally, this approach has been substantiated by Colombie et al. [15] who performed a number of tests with oxide debris formed in situ, debris introduced artificially and open-and-shut tests where the oxide debris was periodically removed. They found that the fretting wear behaviour depended critically on the formation of a debris bed, and that identical wear behaviour was found, independent of the primary body materials, once the debris bed had formed. Iwabuchi et al. [16] conducted fretting tests which mirrored those of Colombie et al. [15], but in this case, oxide particles were artificially supplied to a fretting contact; they concluded that it is the formation of the compacted oxide film that reduces wear in such a contact, and demonstrated that if such a stable layer does not develop, then the addition of oxide particles to the contact can increase the wear rate by promoting abrasion. In similar work examining a sliding wear contact, Kato and Komai [17] again found that supplying oxide particles into the contact could either reduce or increase the wear rate depending on whether a stable debris bed formed.

The successful formation of a load-bearing debris bed is dependent on the balance between the breakdown and ejection of any existing debris bed and the consolidation of new debris into that bed. Jiang et al. [18] proposed that inter-particle adhesion forces predicted by the JKR model [19] are sufficient to explain the formation of protective debris beds from individual debris particles. They suggested that as the temperature is raised, the surface free energy of the debris particles increases, following an Arrhenius relationship (with $E_a \approx 12$ kJ mole^{-1}). As such, increasing temperature results in an increase in the strength of adhesion between debris particles (and thus the stability of the layer) and will promote the incorporation of larger particles into the film and thus increase the rate of its formation.

Sintering is an activation energy dependent process and is generally classed as being significant at a temperature above approximately half of the absolute melting temperature of the material [20]. However, in a tribological contact, the sintering process is seen to be modified by the local conditions. Adachi and Kato [21] demonstrated experimentally that tribo-sintering of alumina wear particles is possible at high test temperatures of 900 °C (a temperature much lower than normally associated with sintering of alumina), with Kato [22] and Kato and Komai [17] demonstrating sintering (in the form of neck growth) between 300 nm Fe_2O_3 particles at room temperature when these particles were supplied to a sliding interface. Additionally, it was found that the wear behaviour of these contacts was governed by the sintering rate of the supplied particles, which was related to their oxygen diffusivity and diameter. Oxides which exhibited higher rates of diffusion showed accelerated tribofilm formation and thus a more rapid transition to mild wear. In the case of Fe_2O_3, it was demonstrated that smaller particles were sintered more easily (and thus promoted the transition to mild wear) whilst larger particles did not sinter and actually increased the rates of wear of the contacts to which they were added [17,22]. This sintering of oxide particles at ambient temperatures in tribological contacts will be accelerated both by the conditions within the contact and also by the fact that the oxide debris particles produced are themselves very small: oxide debris resulting from fretting has been reported to be < 5 nm in diameter [23].

It has been demonstrated that even without any tribological action, the rate of sintering is highly dependent upon the particle size; in early theoretical work, Herring [24] demonstrated that for sintering via surface diffusion, a reduction in particle size by a factor of 10 would result in a reduction in time to the same degree of sintering by a factor of 10^4. Such an increase in rate indicates that nano-particles are expected to sinter at much lower temperatures than larger particles; for example, recent work [25] on uranium dioxide demonstrated sintering of nano-particles at 500 °C–600 °C, some 700 °C–1000 °C below the normal sintering temperatures of bulk uranium dioxide. There is a wider body of research concerning low temperature sintering of metallic nano-particles where sintering of metals has been observed at temperatures around ambient; for example, Zhou et al. [26] investigated the sintering behaviour of a range of ultra-fine powders, and observed that sintering of iron particles (30 nm to 40 nm) initiated as soon as the temperature was increased above 20 °C.

At elevated temperatures (under both fretting and sliding wear conditions), workers have reported the formation of a 'glaze' in the worn contact [1,2,9]. This is often described as a smoothly burnished layer forming on top of a compacted oxide layer. It was originally thought that these glazes were silicon-rich due to their glassy appearance [7]; however, it is now known that they in fact consist of compacted sub-micron size oxide particles [7]. Furthermore, Stott and Wood [7] proposed that the glaze formed as a result of plastic flow of the oxide which was possible due to the small size of the asperity contact and hydrostatic loading conditions present in the tribo-film; more recent publications point to glaze formation being associated with the completion of the sintering process [9,17].

To date, much of the research reported in the literature relating to fretting behaviour at elevated temperature has naturally focused on stainless steels. There appears to be consistent experimental evidence that the transition in fretting wear and COF occurs at ≈200 °C for such steels [1,2]. However, similar investigations involving carbon steels are less conclusive. Kayaba and Iwabuchi [2] reported the transition temperature to be 200 °C for a 0.45 wt % C steel. However, examination of the data indicates that the wear had dropped to about 1/3 of its room temperature value at 100 °C and was small (but still positive) at 200 °C, while becoming negative at all temperatures > 200 °C. In contrast, Hurricks [4] found a gradual decrease in the fretting wear of a mild steel (EN3B) up to 150 °C followed by a more rapid drop until 200 °C. Moreover, despite their widespread use in industrial contacts prone to fretting at elevated temperatures (such as in aero-engine spline couplings), there are no reports in the literature concerning elevated temperature fretting of high strength alloy steels: work with such steels has more generic applicability since it is known that substrate strength can significantly affect the formation and stability of the glaze layer [27], and thus the tribology of the contact. Furthermore, it has been suggested that the transition temperature is dependent on the chromium content of the steel alloy [4,11] (associated with the fact that alloying of the oxide will affect both its rate of formation and its sintering behaviour due to differences in physical properties); many high strength steels have chromium contents between those of the mild steels and stainless steels which have been the subjects of fretting at elevated temperature reported in the literature.

In modern engineering assemblies, particularly modern gas-turbines, wearing parts utilising high strength alloy steels often experience operational temperatures spanning the range previously suggested for the fretting transition temperature. As such, it is important to understand the fretting response of such steels at elevated temperatures. The aim of this work is to characterise and understand the high temperature fretting wear behaviour of one such steel, Super-CMV [28].

2. Experimental method

2.1. Materials and specimens

All specimens were manufactured from a high strength alloy steel – Super-CMV (SCMV) – typically employed in aero-engine

Table 1
Composition of SCMV (wt%) [29].

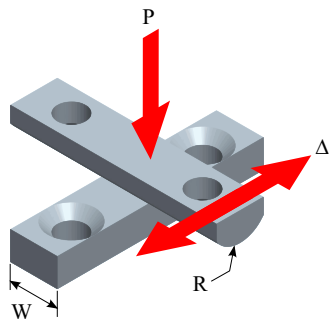| C	Si	Mn	P	S	Cr	Mo	Ni	V	Fe
0.35–0.43	0.1–0.35	0.4–0.7	< 0.007	< 0.002	3.0–3.5	0.8–1.1	< 0.3	0.15–0.25	Remainder

Fig. 1. Diagram of the specimens and their arrangement in the fretting test: $W = 10$ mm, $R = 6$ mm, $P =$ normal load, and $\Delta =$ applied displacement.

transmission components [28]; the composition of the steel is given in Table 1.

The test material was first cut into blanks with a machining allowance on all dimensions. The blanks were heated to 940 °C and held for 45 min, after which they were oil quenched. Subsequently, they were tempered at 570 °C for 120 min and finally air cooled. After grinding to final dimensions (Fig. 1), the Vickers hardness (HV20) of the surface was found to be in the range 4.56 GPa–4.68 GPa, confirming that the decarburised layer had been completely removed.

Elevated temperature nano-indentation testing was conducted by Micro Materials Ltd. (Wrexham, UK) in order to characterise the hardness of the test material as a function of temperature. A heated cubic boron nitride Berkovich indenter was used and the maximum indentation depth was ≈1.1 μm. During the indentation tests, the loading and unloading periods were 20 s, with a 30 s dwell at peak load. Thermal drift was corrected over a period of 120 s at 90% unloading for elevated temperatures, and over a period of 60 s at ambient temperatures. Further information on the procedure and analysis can be found in the literature [30,31].

2.2. Fretting tests

Fretting tests were conducted using a cylinder-on-flat arrangement (Fig. 1), generating a 10 mm line contact. A schematic diagram of the rig is given in Fig. 2. The flat specimen was attached to the static lower specimen mounting block (LSMB) and the cylindrical specimen to the moving upper specimen mounting block (USMB). An oscillatory displacement, Δ (of amplitude Δ^*), and a fixed frequency of 20 Hz was applied to the USMB by an electromagnetic shaker. The relative displacement between the USMB and LSMB was measured by a linear variable differential transformer (LVDT). A constant normal load, P, was applied to the USMB via a dead weight and lever arm. The tangential traction forces were measured using a piezoelectric load cell between the electromagnetic shaker and the USMB. Cartridge heaters were integrated into both the USMB and LSMB with thermocouples located above and below the specimens; independent control loops exist for the heaters in the USMB and LSMB. This arrangement ensured that no thermal gradient existed across the specimen pair. An additional thermocouple was spot welded onto the surface of the flat specimen in order to monitor the temperature near to the contact; in all tests, the deviation between the surface temperature and the heater block temperature was relatively small (less than 1.5 °C at 85 °C and less than 3.5 °C at
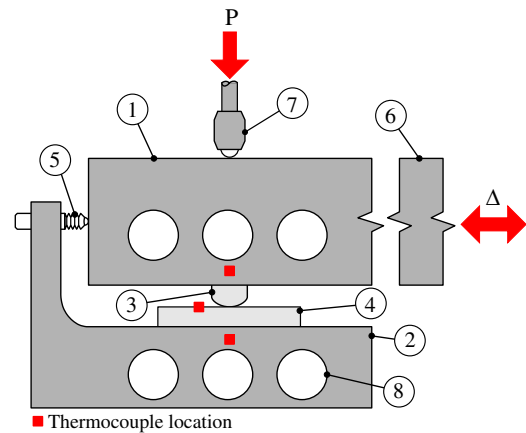

■ Thermocouple location

Fig. 2. Schematic diagram of the fretting rig: (1) moving upper specimen mounting block (USMB), (2) fixed lower specimen mounting block (LSMB), (3) cylindrical specimen, (4) flat specimen, (5) LVDT, (6) load cell, (7) normal-load rod, and (8) cartridge heaters.
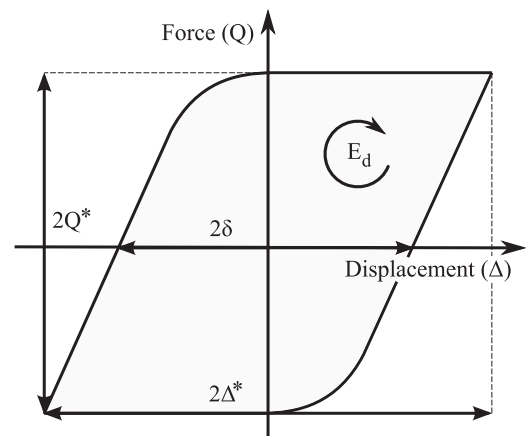

Fig. 3. Diagram of a gross sliding fretting loop with the key parameters indicated: Q, tangential force; Δ, applied displacement; Q^*, tangential force amplitude; Δ^*, applied displacement amplitude; δ, sliding amplitude; and E_d, dissipated energy.

Table 2
Fretting test conditions.

Normal load	P (N)	250
Applied displacement	Δ^* (μm)	25
Duration	N (cycles)	100 000
Frequency	f (Hz)	20
Temperature	T (°C)	24, 85, 120, 150, 300, 450

450 °C). Before testing, the specimens were thoroughly degreased using detergent and industrial methylated spirit.

The control and data acquisition system, written in Lab-VIEW™, continuously recorded the tangential force and relative displacement at 4 kHz sampling rate, whilst the thermocouples were sampled at 1 Hz. The control system continuously modulated the signal sent to the electromagnetic shaker in order to maintain a constant value of Δ^*. Post-processing of the data enabled important quantitative fretting parameters to be derived such as

the sliding amplitude, δ, the tangential force amplitude, Q and the dissipated energy, E_d; Fig. 3 shows an idealised, gross sliding, force-displacement fretting loop with the significant parameters labelled. The sliding amplitude, δ, was determined as the residual displacement when $Q=0$. Since the data were recorded continuously, it was possible to derive these parameters for every cycle throughout the test. The fretting conditions used in this study are summarised in Table 2.

2.3. Characterization of wear

A tactile profilometer (Taylor-Hobson Talysurf CLI 1000) with a fine diamond stylus (90°, 2 µm radius) was used to measure the surface profile of the worn specimens. Prior to scanning, the specimens were rinsed with industrial methylated spirit to remove any debris not adhered to the surface. As the wear scars extend over the full width of the flat specimens, profiles were taken over only the central 8 mm of the scars at 0.25 mm spacing between traces. For the cylindrical specimen, similarly spaced profiles were taken over an area completely spanning the wear scar.

In order to estimate the wear volume, a reference (unworn) surface must be defined. In the case of the flat specimen, the reference surface was defined as the best fit plane to all points outside of the wear scar. However, definition of the reference surface is more difficult for the cylindrical specimen. When conducting the profilometry, it was ensured that the first and last profiles were always entirely outside of the worn area. A polynomial fit was then taken for these two profiles and an estimate for the unworn surface was generated by interpolating between these two fitted profiles — illustrated by the mesh in Fig. 4. Any material build-up above the reference plane (for either the flat or cylindrical specimen) is
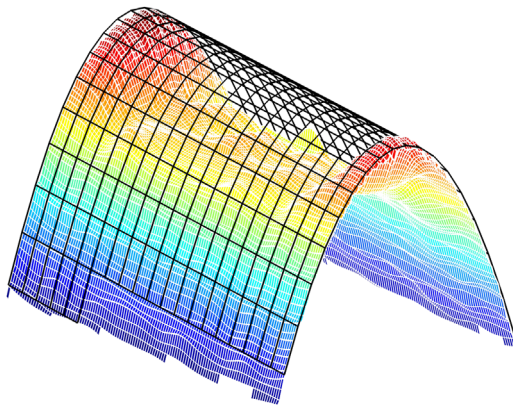
considered to be transferred material or debris, and is defined by a positive volume (V^+); any loss of material from below the reference plane is defined as a negative volume (V^-) (see Fig. 5). The overall wear volume (V^w) is then defined as follows:

$$V^+ = V^+_{cylinder} + V^+_{flat} \qquad (1a)$$

$$V^- = V^-_{cylinder} + V^-_{flat} \qquad (1b)$$

$$V^w = -(V^+ + V^-) \qquad (1c)$$

Scanning electron microscopy (SEM) was used to produce micrographs of a number of wear scars in both plan and sectional view. This allowed a qualitative examination of any features indicated by the profilometry. The specimens which required sectioning were cut on a diamond wheel, mounted and polished, then etched with 2% nital for 15 s. In the SEM, secondary electron imaging (SEI) and back-scattered electron image (BEI) were used, with the latter differentiating between materials of different average atomic number, allowing clear distinction to be made between substrate and wear debris for example. Further chemical characterization was achieved using energy dispersive X-ray spectroscopy (EDX).

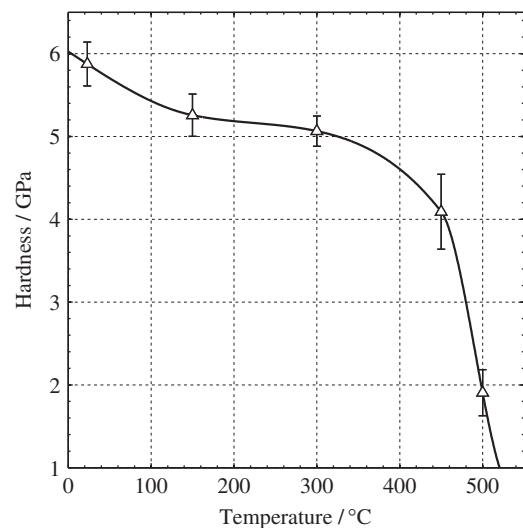**Fig. 4.** Schematic diagram of a worn surface and the fitted reference surface (mesh).
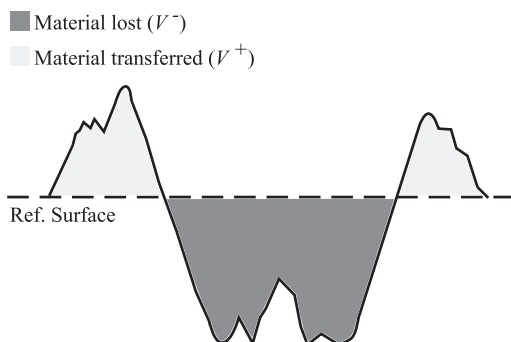
Fig. 5. Schematic diagram indicating the assessment of transfer (V^+) and wear (V^-) volume.

Fig. 6. Nano-indentation hardness of SCMV as a function of temperature.
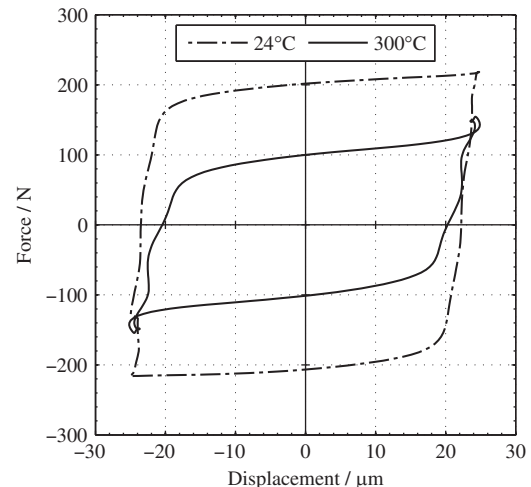
Fig. 7. Force-displacement loops for fretting tests conducted at 24 °C and 300 °C taken at 50×10^3 cycles.
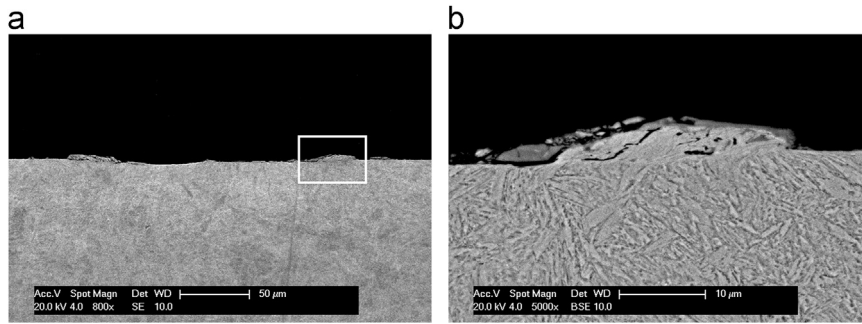
Fig. 8. SEM micrographs, showing ploughing of metallic material at the edge of the wear scar, following a test at 300 °C which showed force peaks at the extremes of the stroke: (a) low magnification image of the whole scar and (b) higher magnification image of the region highlighted in (a).
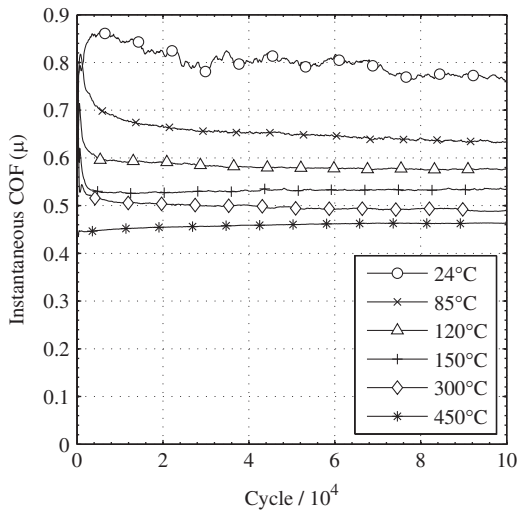

Fig. 9. Development of the COF with cycle count during fretting as a function of temperature.
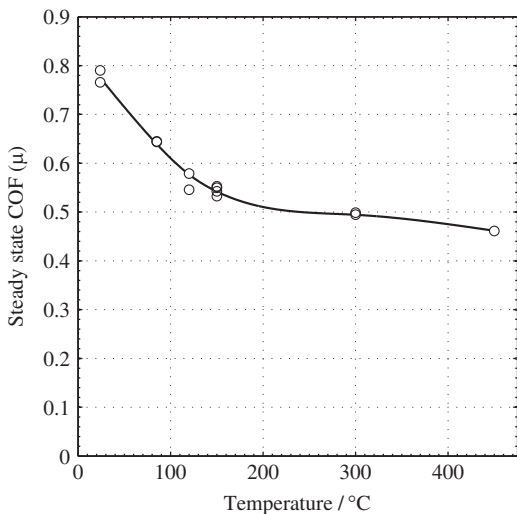

Fig. 10. Relationship between the steady state COF and temperature (steady state COF represents the average of the values recorded in the fretting tests from 25×10^3 to 100×10^3 cycles).

Fig. 11. Relationship between wear and temperature of fretting: (a) net wear volume and (b) constituent material build-up and removal volumes.

3. Experimental results

The relationship between hardness and temperature is shown in Fig. 6. It can be seen that there was little material softening until 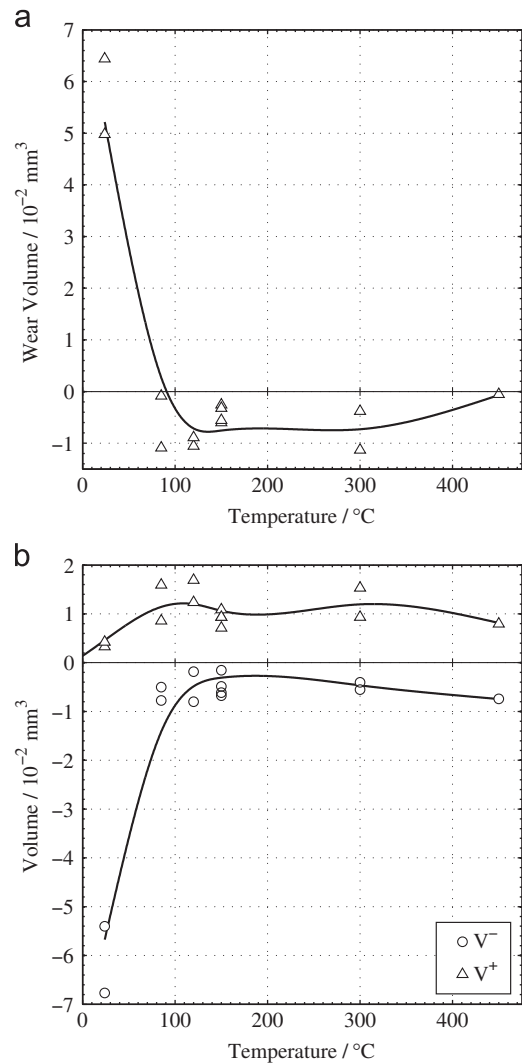the region of 300 °C–450 °C, whereupon the hardness began to decrease sharply. The hardness fell by ≈14% on raising the temperature from room temperature to 300 °C, with the decrease reaching ≈30% by 450 °C.

All fretting tests conducted below 300 °C showed classic parallelogram force-displacement loops indicative of gross sliding (Fig. 3). However, loops from some tests conducted at temperatures ≥300 °C exhibited distinctive force peaks at the extremes of the stroke, Δ^* (Fig. 7). Such features have previously been reported during the

fretting of ductile materials [32,33], and also during high temperature fretting of a stainless steel [1]. They are believed to be caused by ploughing at the edges of the contact leading to a build-up of material in that area [32]. Subsequent interaction between the moving specimen and the built up material then results in the observed force peaks. Cross-sectioning and SEM examination (Fig. 8) of a specimen where this behaviour was observed clearly show a significant build-up of highly plastically deformed metallic material at the extreme edges of the wear scar. As a consequence of this behaviour, the normalised tangential force ratio (Q^*/P) is no longer an effective estimate of the COF. Fouvry et al. [32] have proposed an estimate for the COF (μ_e, Eq. (2)) based on the dissipated energy per cycle which is less sensitive to such behaviour. Throughout the remainder of this work, μ_e is used as the definition of the COF.

$$\mu_e = \frac{E_d}{4P\delta} \qquad (2)$$

Fig. 9 shows the development of the COF with time for fretting tests conducted under each of the temperatures examined. It was observed that at 24 °C, the COF rapidly rose to a maximum of 0.86 at approximately 6×10^3 cycles, before gradually dropping to 0.8 at 24×10^3 cycles, where it may be considered to have reached a quasi-stable value. Whilst quasi-stable, the COF displayed notable variation over a period of hundreds of cycles and continued to do so throughout the test. In contrast, at 85 °C, the COF declined rapidly from an initial peak of 0.82 at 500 cycles, reaching a value

of 0.68 by 20×10^3 cycles. Subsequently, the COF assumed its quasi-stable value and was contrastingly stable over a period of hundreds of cycles. As the temperature was further increased, the COF became more stable, and the minimum (quasi-stable) value was reached following a smaller number of cycles; at 150 °C, the steady value of COF was 0.62, with this value being reached in 12×10^3 cycles. At the highest temperature studied (450 °C), there was no discernible initial peak in the COF and the steady state value was immediately attained.

In order to quantitatively compare the dependence of the COF on temperature, the last 75×10^3 cycles of each test were averaged to produce a quasi-steady state COF value (Fig. 10). Data for repeat tests are plotted and it is apparent that variation in the COF readings was small (< 0.04). It can be seen that the steady state COF drops monotonically with increasing temperature from 0.78 at 24 °C to a minimum of 0.46 at 450 °C. The observed rate of change of the COF is initially fast, dropping from 0.77 at 24 °C to 0.64 at 150 °C; however, above 150 °C the rate of change reduces significantly.

The relationship between temperature and total wear volume is plotted in Fig. 11 (a); it is observed that in the temperature interval 24 °C–85 °C, the wear response altered from one of net volume loss to net volume gain (such volume gains are small and are associated with the fact that both Fe_2O_3 and Fe_3O_4 have Pilling–Bedworth ratios of greater than two [34]). Fig. 11 (b) decomposes the wear volume into its constituent volumes, V^- and V^+. It is apparent that the decrease in wear volume on increasing the temperature from
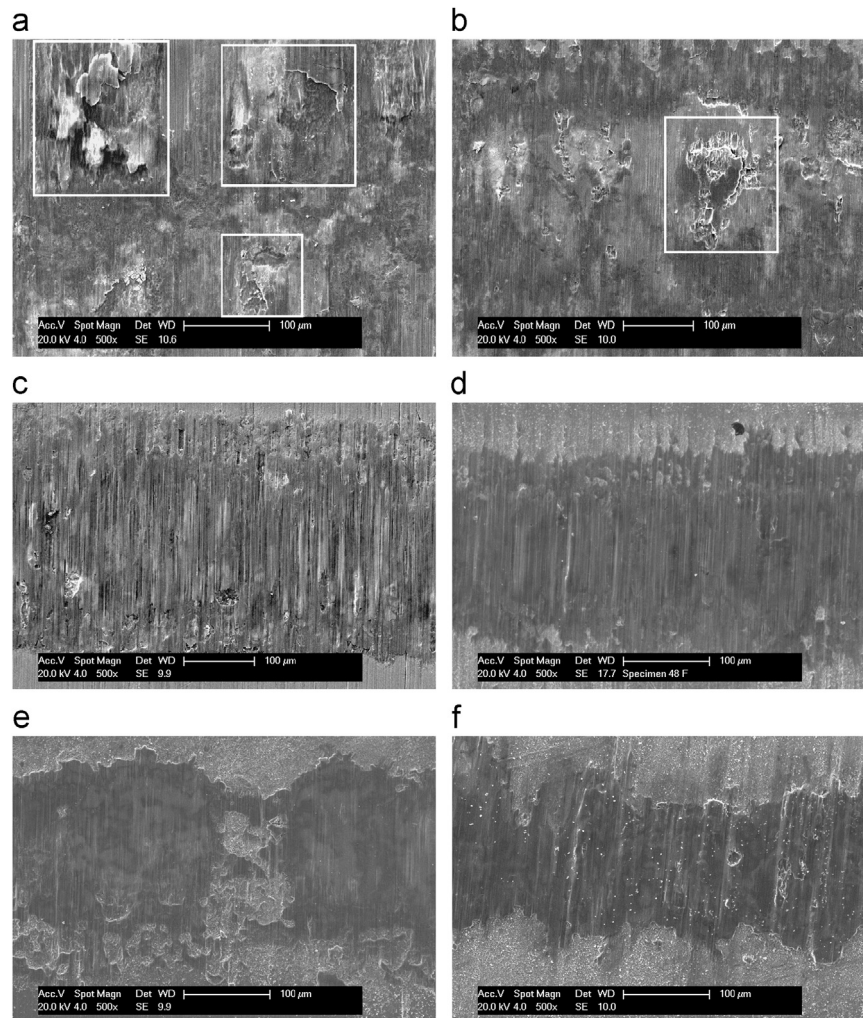

Fig. 12. Secondary electron SEM plan-view micrographs of wear scars on the flat specimen following fretting at a range of temperatures: (a) 24 °C, (b) 85 °C, (c) 120 °C, (d) 150 °C, (e) 300 °C, (f) 450 °C; areas of debris-bed breakdown and flake formation are highlighted in (a) and (b).
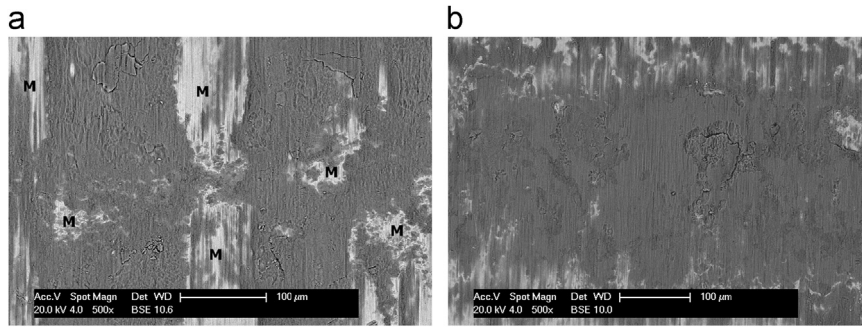
Fig. 13. Back-scattered electron SEM plan-view micrographs of the wear scar on the flat specimen following fretting at (a) 24 °C and (b) 85 °C. The areas of the fretting contact where an oxide-based debris bed has not formed are indicated with an 'M'.
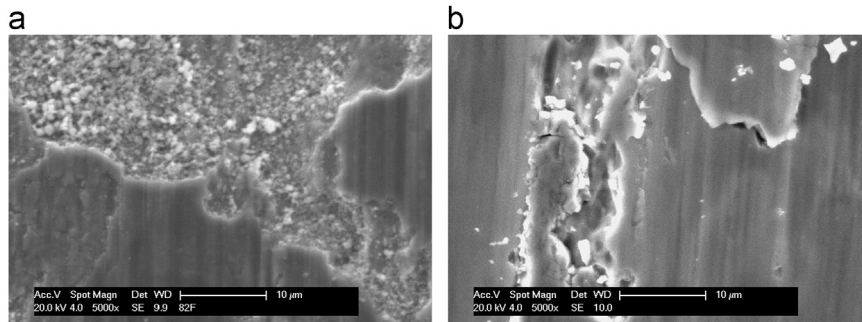

Fig. 14. SE-SEM micrographs of significant 'glaze' formation on the surface of oxide beds on the flat specimen following fretting at (a) 300 °C and (b) 450 °C.

ambient to 85 °C was due to a sudden, and large (87%), decrease in the volume of material lost (V^-), concurrent with a smaller increase in the amount of additional material built up on the surfaces (V^+). There is no evidence of significant material transfer between the two members of the fretting couple having occurred; such a situation would be indicated by similarly sized volumes of material removed and material built up within the contact. As the temperature was increased above 85 °C, there were no further notable changes in the wear response, and the behaviour remained one of low material removal and additional material build up on the surface, resulting in small negative total wear volumes (i.e. increases in total volume). This relative insensitivity of wear volume to temperature is in contrast to the changes in the COF, which continued to drop significantly as the temperature was increased to 450 °C.

Qualitative assessment of the wear scars was made using SEM. Fig. 12 shows a plan view secondary-electron (SE) micrograph of a flat specimen for each temperature studied. At 24 °C, the debris bed exhibited a roughened appearance, with large flakes of oxide being apparent (Fig. 12a); examination using back-scattered-electron imaging (BSI) (Fig. 13a) indicates that the compacted oxide debris (regions of lower contrast) only partially covered the wear scar, with relatively large areas of metal remaining exposed. In contrast, at 85 °C, the compacted oxide debris exhibited almost total coverage of the scar (Fig. 13b) and was much smoother in appearance, although there were still areas where delamination and breakdown of the oxide had occurred (Fig. 12b). As the temperature was increased further to 120 °C, the surface of the compacted oxide formed appears smoother still (Fig. 12(c)), whilst following fretting at 150 °C, the surface appears glassy and burnished and may be described as a 'glaze-layer' (Fig. 12d). At 300 °C and 450 °C, the evolution of the glaze was complete, with large islands of smooth polished oxide on the surface of oxide debris (Fig. 12e–f); Fig. 14 shows higher magnification detail of some of these smooth glazes at 300 °C and 450 °C. A cross section through the glaze layer (Fig. 15) indicates that the glaze was composed of finely divided oxide debris which had been compacted to form the bed.
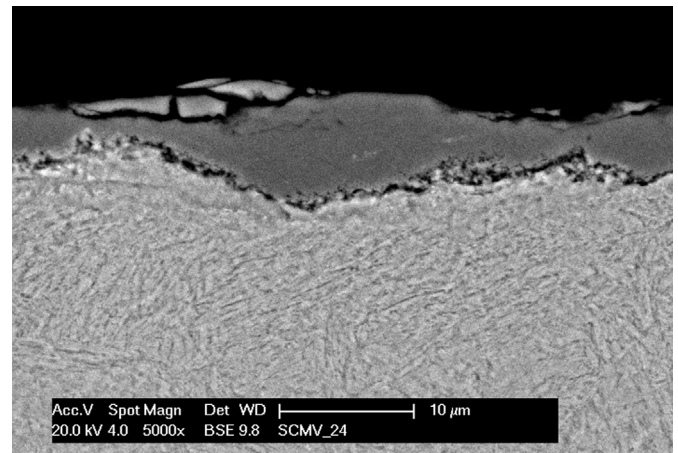

Fig. 15. Back-scattered electron micrograph cross-section through the surface glaze formed following fretting at 450 °C.

As the temperature of fretting was increased above room temperature, not only are changes in the nature of coverage of the oxide debris beds observed, but it is also observed that the width of the wear scar (and hence contact area) decreased (as a result of the reduction in wear rate). This effect is quantified in Fig. 16. It can be seen that, initially, the width dropped rapidly with increasing temperature up to 150 °C, decreasing to ≈0.26 mm from the 0.63 mm observed following room temperature fretting; increasing the temperature further to 450 °C resulted in only a relatively small additional reduction to 0.16 mm.

In order to evaluate the endurance of the glaze layer structures observed in the SEM (Fig. 12), a test was run with a variable temperature. The temperature was initially set at 300 °C and the test was allowed to proceed normally for 50×10^3 cycles, at which point, the test was automatically stopped, and the rig was left to
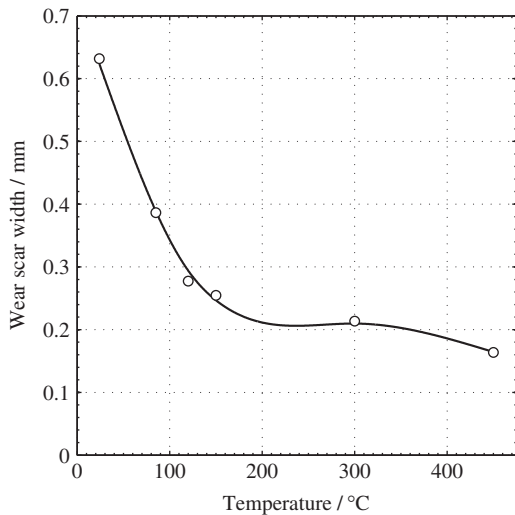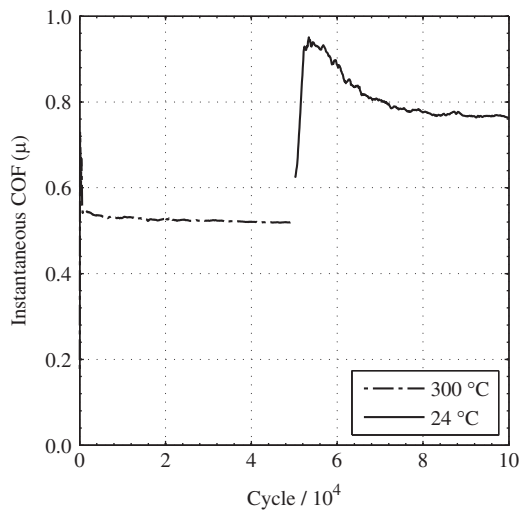
Fig. 16. Wear scar width as a function of temperature.

Fig. 17. Coefficient of friction as a function of cycles for a test run at 300 °C for 50×10^3 cycles and then at 24 °C for a further 50×10^3 cycles.

cool with the specimens in place. When the rig had cooled to ambient temperature, the test was restarted and continued for a further 50×10^3 cycles. The resulting COF as a function of cycles is shown in Fig. 17. It can be seen that the initial behaviour (dashed line) is in close agreement with that previously observed at 300 °C (Fig. 9). On resumption of the test at 24 °C (solid line), it can be seen that the COF climbs rapidly to a maximum of ≈0.95 in a period of 3400 cycles from the test restarting. By the end of the test, the COF had stabilised at a similar steady-state value to those previously observed for tests conducted at ambient temperatures. On completion of the test, a large amount of characteristic red-oxide was observed, similar to that observed following tests run at ambient temperature rather than those run at or above 85 °C, which showed limited production of oxide debris.

4. Discussion

It is clear that a significant modification of the wear behaviour of SCMV occurred in the temperature interval between 24 °C and 85 °C. While bulk material removal was observed at room

temperature, at 85 °C there was 'negative' wear i.e., the volume of material built up on the surfaces was greater than the volume of material removed. This behaviour was not amplified by further increasing the temperature, and the wear volume remained approximately constant (and small). While the transition temperature is in agreement with the value that Kayaba and Iwabuchi [2] reported for a 0.45 wt% C steel fretting at a much higher amplitude of 150 μm, the behaviour at the transition appears to show a different evolution. Kayaba and Iwabuchi [2] observed the wear rate of the steel to initially drop rapidly between 80 °C and 100 °C and then more progressively until 200 °C, whereupon the wear became negative. At this temperature, the initiation of significant adhesive transfer of the oxide layer was found to occur. In the current work, negative wear was observed at all elevated temperatures examined, but no evidence of material transfer was found. SEM examination of the scars (Fig. 15) indicates that the formation of the debris bed resulted from accumulation and retention of finely divided oxide debris within the contact. Additionally, the profilometry results (Fig. 11(b)) indicate that there was no initiation of any adhesive transfer, which if it were occurring, would be indicated by an increase in the V^+ and V^- volumes (although not necessarily by any change in the overall wear volume).

Observation of the SEM micrographs (Fig. 12) indicates that as the wear rates fell with increasing temperature, there was an associated change in the appearance of the debris bed formed within the contact. Following fretting at 24 °C, the debris bed was rough in appearance with large areas in the process of delamination and breakdown (Fig. 12(a)); in addition, significant areas of exposed metal were visible across the wear scar (Fig. 13(a)). In contrast, at 85 °C, the surface of the wear scar was smoother and the oxide exhibited a more complete coverage of the scar. Whilst there were still areas of the debris bed undergoing breakdown, those areas were less prevalent. This trend continued with increasing temperature; at 300 °C, the debris bed surface was generally very smooth and burnished – consistent with the typical description of a 'glaze-layer'. High magnification examination of the smooth areas shows them forming on the surface of fine granular oxide beds (Fig. 14). Whilst this evolution may be observed qualitatively in the SEM micrographs, plotting the width of the wear scar (Fig. 16) provides a quantitative analysis. It can be seen that the width of the wear scar dropped by 40% between 24 °C and 85 °C—this is mainly attributed to the reduction in wear. However, at temperatures higher than 85 °C, the wear volume remained approximately constant and the width of the wear scar continued to decrease, indicating that the load bearing capacity of the established tribo-film was greater at higher temperatures. At the highest temperature studied (450 °C), the scar width was 0.16 mm, only twice the initial Hertzian contact width. Similarly, the COF decreased monotonically between 24 °C and 450 °C, but with no commensurate change in the wear rate. Testing to explore the resilience of the glaze-layer formed at high temperatures found it to disperse almost immediately when fretting was resumed at ambient temperature (Fig. 17). Subsequent optical examination of the scar showed it to be similar in appearance to that observed following tests conducted entirely at ambient temperature, with dispersed areas of compressed oxide and visible metal. This effect is in accord with work conducted by Rybiak et al. [1] on the fretting of a stainless steel under variable temperature conditions.

As outlined in the Introduction, changes in temperature will affect the formation and properties of the oxide bed primarily through changes to the rate of oxidation or changes to the way that individual debris particles are either formed into a load-bearing bed (through changes both to the adhesion forces between particles and changes in the kinetics of sintering) or ejected from

the contact. Additionally, the bulk steel properties may be sufficiently changed at elevated temperatures to influence the wear process, or affect the formation of a stable load-bearing bed. Whilst all of these will clearly influence the tribology of the contact, it is important to understand which is the primary cause of the changes observed.

Fig. 6 indicates that increases in temperature above ambient have a relatively small effect (less than $\approx 14\%$) on the hardness until temperatures greater than 300 °C, a temperature significantly higher than the 24 °C–85 °C temperature interval over which the wear rate was observed to fall rapidly. As such, it may be concluded that changes in the mechanical properties of the substrate are not the cause of the transition in wear. However, the marked material softening above 300 °C does coincide with the slight increase in wear at 450 °C (Fig. 11(a)).

There is general agreement in the experimental literature that the frictional work done does not significantly influence the macroscopic temperature of the contact [35,36]. However, modelling has indicated that high flash temperatures (> 1000 °C) may exist at asperities which would be expected to influence the evolution of the debris bed [37,38]. Experimental evidence and modelled predictions indicate that the resulting thermal fields extend in the order of microns; it has been shown that over 90% of the frictional energy is dissipated within 5 μm of the surface [39,40]. These surface flash temperatures may be one of the reasons why oxide debris is observed at such low temperatures in any fretting contact; however, the effect of these flash temperatures does not (in itself) explain the change in behaviour on raising the bulk temperature from room temperature to 85 °C.

Hurricks [4,5] suggested that increases in temperature above ambient affected the tribology of fretting contacts primarily through a change in oxidation kinetics. The change in oxidation rate for iron from logarithmic to parabolic behaviour is known to occur at approximately 200 °C [41], which is significantly higher than the temperature of the transition in wear behaviour observed in the current tests (85 °C). As such, it seems unlikely that the specimen surface oxide film can spontaneously grow to a critical thickness at these lower temperatures. Additionally, if the transition were due to a change in the oxide from $\alpha-Fe_2O_3$ to Fe_3O_4, (the latter being thought to act as a better solid lubricant), then it would be anticipated that the trends observed in the measured COF as a function of temperature would mirror the changes in the wear rate; this is not observed, with the wear rate changing little between 85 °C and 300 °C, whereas the COF continued to decline over the same temperature range. In fretting experiments on stainless steel over a range of temperatures, Rybiak et al. [1] concluded that the transition in wear behaviour was due to the tribo-sintering process demonstrated by Kato and Komai [17] and Kato [22]. In the current experiments, this also seems the most likely explanation for the significant reduction in rate of wear between 24 °C and 85 °C. The sudden drop in wear between these temperatures occurred simultaneously with a significant reduction in the amount of ejected oxide debris and a noticeable change in character of the wear scar (Fig. 12). There seems to be a critical temperature at which the adhesion between the oxide debris particles becomes sufficient to inhibit their independent removal from the contact and thus results in the formation of a stable load bearing tribofilm. As a result, the wear rate reduces dramatically; likewise, increasing the coverage of the oxide debris bed within the contact reduces the number of interactions between metallic-asperities resulting in a reduction in COF. As the temperature is raised, the JKR adhesive forces [19] will be stronger between individual debris particles (reducing their tendency for ejection from the contact), and the rate of sintering will increase (meaning that a stable debris bed is formed), both resulting in a more rapid development of the protective bed. This is reflected in the time

evolution of the COF in individual tests (Fig. 9), where the steady state was seen to be attained more quickly at higher temperatures. As the sintering became more complete, so the load capacity of the debris bed increased, resulting in a reduction in wear scar width with temperature (Fig. 16). The monotonic decrease in COF with temperature in the range 24 °C–450 °C is commensurate with the increasingly glaze-like appearance of the worn surface (Fig. 12).

5. Conclusions

From the fretting wear testing completed for Super-CMV at temperatures from 24 °C–450 °C in air the following conclusions can be drawn:

1. The fretting wear of SCMV is strongly influenced by temperature and a significant reduction in wear is found between 24 °C and 85 °C.
2. The reduction in wear is due to the retention of wear debris within the scar leading to the formation of a stable-load bearing bed and eventually a 'glaze-layer'. The results support the view that this is due to a tribo-sintering process as described by Kato and Komai [17].
3. The coefficient of friction is found to be strongly dependent on temperature and decreases continuously from 0.78 to 0.46 between 24 °C and 450 °C.
4. The reduction in coefficient of friction is found to be commensurate with the progressive formation of a 'glaze-layer'.
5. The results show good mechanistic agreement with those found by Rybiak et al. [1] for a stainless steel. However, the temperature of the transition between the high wear rate and low wear rate regimes was at a much lower temperature, and indicates the importance of understanding the effect of temperature on the fretting of steels which are more prone to oxidation than stainless steels.

References

[1] R. Rybiak, S. Fouvry, B. Bonnet, Fretting wear of stainless steels under variable temperature conditions: introduction of a 'composite' wear law, Wear 268 (2010) 413–423.
[2] T. Kayaba, A. Iwabuchi, The fretting wear of 0.45% C steel and austenitic stainless steel from 20 to 650 °C in air, Wear 74 (1981) 229–245.
[3] D.E. Taylor, F.B. Hardisty, R.B. Waterhouse, A.Y. Nehru, The fretting wear of an austenitic stainless steel in air and in carbon dioxide at elevated temperatures, Wear 56 (1979) 9–18.
[4] P.L. Hurricks, Fretting wear of mild-steel from room-temperature to 200 °C, Wear 19 (1972) 207–229.
[5] P.L. Hurricks, Fretting wear of mild-steel from 200 °C to 500 °C, Wear 30 (1974) 189–212.
[6] H.H. Uhlig, I.M. Feng, W.D. Tierney, A. McClellan, A fundamental investigation of fretting corrosion, Technical Note 3029, NACA, 1953.
[7] F.H. Stott, G.C. Wood, The influence of oxides on the friction and wear of alloys, Tribology International 11 (1978) 211–218.
[8] F.H. Stott, J. Glascott, G.C. Wood, The sliding wear of commercial Fe-12%Cr alloys at high temperature, Wear 101 (1985) 311–324.
[9] F.H. Stott, High-temperature sliding wear of metals, Tribology International 35 (2002) 489–495.
[10] J. Glascott, G.C. Wood, F.H. Stott, The influence of experimental variables on the development and maintenance of wear-protective oxides during sliding of

high-temperature iron-base alloys, Proceedings of the Institution of Mechanical Engineers—Part C: Mechanical Engineering Science 199 (1985) 35–41.

[11] W.T. Clark, C. Pritchard, J.W. Midgley, Mild wear of unlubricated hard steels in air and carbon dioxide, Proceedings of the Institution of Mechanical Engineers, Conference Proceedings 182 (1967) 97–105.

[12] R.T. Foley, M.B. Peterson, C. Zapf, Frictional characteristics of cobalt, nickel, and iron as influenced by their surface oxide films, ASLE Transactions 6 (1963) 29–39.

[13] M. Godet, The third-body approach: a mechanical view of wear, Wear 100 (1984) 437–452.

[14] Y. Berthier, L. Vincent, M. Godet, Velocity accommodation in fretting, Wear 125 (1988) 25–38.

[15] C. Colombie, Y. Berthier, A. Floquet, L. Vincent, M. Godet, Fretting—load carrying capacity of wear debris, Journal of Tribology 106 (1984) 194–201.

[16] A. Iwabuchi, K. Hori, H. Kubosawa, The effect of oxide particles supplied at the interface before sliding on the severe-mild wear transition, Wear 128 (1988) 123–137.

[17] H. Kato, K. Komai, Tribofilm formation and mild wear by tribo-sintering of nanometer-sized oxide particles on rubbing steel surfaces, Wear 262 (2007) 36–41.

[18] J. Jiang, F.H. Stott, M.M. Stack, The role of triboparticulates in dry sliding wear, Tribology International 31 (1998) 245–256.

[19] K.L. Johnson, K. Kendall, A.D. Roberts, Surface energy and the contact of elastic solids, Proceedings of the Royal Society of London-Series A, Mathematical and Physical Sciences 324 (1971) 301–313.

[20] R.M. German, Sintering Theory and Practice, John Wiley & Sons (A Wiley-Interscience Publication), 1996.

[21] K. Adachi, K. Kato, Formation of smooth wear surfaces on alumina ceramics by embedding and tribo-sintering of fine wear particles, Wear 245 (2000) 84–91.

[22] H. Kato, Effects of supply of fine oxide particles onto rubbing steel surfaces on severe–mild wear transition and oxide film formation, Tribology International 41 (2008) 735–742.

[23] R.C. Bill, Review of the factors that influence fretting wear, in: S.R. Brown (Ed.), Materials Evaluation Under Fretting Conditions, ASTM Special Technical Publication, vol. 780, ASTM, 1982, pp. 165–182.

[24] C. Herring, Effect of change of scale on sintering phenomena, Journal of Applied Physics 21 (1950) 301–303.

[25] T.M. Nenoff, B.W. Jacobs, D.B. Robinson, P.P. Provencio, J. Huang, S. Ferreira, D.J. Hanson, Synthesis and low temperature in situ sintering of uranium oxide nanoparticles, Chemistry of Materials 23 (2011) 5185–5190.

[26] Y.-H. Zhou, M. Harmelin, J. Bigot, Sintering behaviour of ultra-fine Fe, Ni and Fe-25 wt% Ni powders, Scripta Metallurgica 23 (1989) 1391–1396.

[27] R.B. Waterhouse, Fretting at high temperatures, Tribology International 14 (1981) 203–207.

[28] T. Ford, Mainshafts for the Trent, Aircraft Engineering and Aerospace Technology 69 (1997) 555–560.

[29] I.R. McColl, J. Ding, S.B. Leen, Finite element simulation and experimental validation of fretting wear, Wear 256 (2004) 1114–1127.

[30] N.M. Everitt, J. Ding, G. Bandak, P.H. Shipway, S.B. Leen, E.J. Williams, Characterisation of fretting-induced wear debris for Ti-6Al-4V, Wear 267 (2009) 283–291.

[31] N. Everitt, M. Davies, J. Smith, High temperature nanoindentation—the importance of isothermal contact, Philosophical Magazine 91 (2011) 1221–1244.

[32] S. Fouvry, P. Duó, P. Perruchaut, A quantitative approach of Ti-6Al-4V fretting damage: friction, wear and crack nucleation, Wear 257 (2004) 916–929.

[33] T. Dick, C. Paulin, G. Cailletaud, S. Fouvry, Experimental and numerical analysis of local and global plastic behaviour in fretting wear, Tribology International 39 (2006) 1036–1044.

[34] N. Birks, G. Meier, Introduction to High Temperature Oxidation of Metals, Chemistry Series, Edward Arnold, 1983.

[35] E.S. Sproles, D.J. Duquette, Interface temperature-measurements in fretting of a medium carbon-steel, Wear 47 (1978) 387–396.

[36] B.L. Weik, M.J. Furey, B. Vick, Surface temperatures generated with ceramic materials in oscillating fretting contact, Journal of Tribology 116 (1994) 260–267.

[37] M. Kalin, Influence of flash temperatures on the tribological behaviour in low-speed sliding: a review, Materials Science and Engineering A 374 (2004) 390–397.

[38] M. Kalin, J. Viźintin, Comparison of different theoretical models for flash temperature calculation under fretting conditions, Tribology International 34 (2001) 831–839.

[39] F.E. Kennedy, Single pass rub phenomena—analysis and experiment, Journal of Lubrication Technology 104 (1982) 582–588.

[40] F. Vodopivec, J. Viźintin, B. Suśtarśić, Effect of fretting amplitude on microstructure of 1C–1.5Cr steel, Materials Science and Technology 12 (1996) 355–361.

[41] W.H.J. Vernon, E.A. Calnan, C.J.B. Clews, T.J. Nurse, The oxidation of iron around 200 °C, Proceedings of the Royal Society of London-Series A, Mathematical and Physical Sciences 216 (1953) 375–397.